

BRICK1 Is Required for Apical Cell Growth in Filaments of the Moss *Physcomitrella patens* but Not for Gametophore Morphology ^W

Pierre-François Perroud and Ralph S. Quatrano¹

Department of Biology, Washington University, St. Louis, Missouri 63130

When BRK1, a member of the Wave/SCAR complex, is deleted in *Physcomitrella patens* ($\Delta brk1$), we report a striking reduction of filament growth resulting in smaller and fewer cells with misplaced cross walls compared with the normal protonemal cells. Using an inducible green fluorescent protein–talin to detect actin in living tissue, a characteristic broad accumulation of actin is observed at the tip of wild-type apical cells, whereas in $\Delta brk1$, smaller, more distinct foci of actin are present. Insertion of *brk1-yfp* into $\Delta brk1$ rescues the mutant phenotype and results in BRK1 being localized only in the tip of apical cells, the exclusive site of cell extension and division in the filament. Like BRK1, ARPC4 and At RABA4d are normally localized at the tip of apical cells and their localization is correlated with rapid tip growth in filaments. However, neither marker accumulates in apical cells of $\Delta brk1$ filaments. Although the $\Delta brk1$ phenotypes in protonema are severe, the leafy shoots or gametophores are normally shaped but stunted. These and other results suggest that BRK1 functions directly or indirectly in the selective accumulation/stabilization of actin and other proteins required for polar cell growth of filaments but not for the basic structure of the gametophore.

INTRODUCTION

Morphogenesis in plant cells depends on the direction and localization of the processes controlling cell elongation and/or division (Fowler and Quatrano, 1997). The requirement for and localization of an actin network at the tip of polar extending filaments are common features of plant cells undergoing polar elongation (reviewed in Mathur, 2005; Smith and Oppenheimer, 2005). To understand the control of localized elongation and the orientation of cell division in cells of filaments, we have focused our attention on members of the protein complexes that regulate assembly of the actin network (e.g., Arp2/3 and Wave/SCAR complexes; for recent reviews, see Ibarra et al., 2005; Takenawa and Suetsugu, 2007).

Homologs for each member of the animal Arp2/3 and Wave/SCAR complexes (Machesky and Insall, 1998; Mullins and Pollard, 1999) have been reported in seed plants (Deeks and Hussey, 2005), but neither complex has been biochemically isolated from any plant nor have they been localized to any intracellular site in vascular plants. Hence, an understanding of the relationship between the localization of these complexes and the sites of cortical assembly of actin filaments/cables during tip growth and oriented cell division is lacking. However, mutant analyses of members of the Arp2/3 (Szymanski, 2005) and Wave/SCAR (Djakovic et al., 2006; Le et al., 2006) complexes in plants show overlapping and similar functions, while double mutant analysis

confirmed a direct genetic link between the two complexes (Deeks et al., 2004; Basu et al., 2005). None of these mutations were lethal, however, and the cell types most affected were localized primarily to the epidermis: trichomes in *Arabidopsis thaliana* (Szymanski, 2005) and pavement cells in maize (*Zea mays*; Frank et al., 2003), both of which failed to develop their normal shape/pattern. These morphological modifications were correlated with defects in the distribution and patterning of actin filaments but were not coupled to the localization of the Arp2/3 and Wave/SCAR complexes. Interestingly, polar tip growth of root hairs and elongation of the hypocotyl were only slightly affected (Mathur et al., 2003; Li et al., 2004), while no effects were observed in tip growth of pollen tubes (Le et al., 2006). If these complexes are involved in the growth of pollen tubes, the above evidence suggests that mutations in either complex are not lethal or that redundant functions for pollen growth reside in other proteins/mechanisms.

In vitro studies in *Arabidopsis* have shown some of the same interactions of the subunits described in animals and yeast. For example, the C-terminal portions of *Arabidopsis* SCAR2, 3, and 4 are able to activate Arp2/3 nucleation in vitro (Frank et al., 2004; Basu et al., 2005). Within the putative plant Wave/SCAR complex, in vitro interactions have been shown between the N-terminal portion of the same plant SCAR (SHD domain) and both plant BRICK1/HSPC300 (BRK1) and Abi (ABI-1/DIS3) (Frank et al., 2004; Basu et al., 2005; Zhang et al., 2005), between PIR121/SRA1 and Nap125 (Basu et al., 2004; El-Assal et al., 2004) and between PIR121/SRA1 and Abi (Basu et al., 2005). The systematic analysis in *Arabidopsis* of interactions between components of the Arp2/3 complex and the Wave/SCAR complex, using both yeast two-hybrid assay and in planta bimolecular fluorescence complementation (Uhrig et al., 2007), confirmed and detailed these interactions. More specifically, At BRK1/HSPC300

¹ Address correspondence to rsq@wustl.edu.

The author responsible for distribution of materials integral to the findings presented in this article in accordance with the policy described in the Instructions for Authors (www.plantcell.org) is: Ralph S. Quatrano (rsq@wustl.edu).

^WOnline version contains Web-only data.

www.plantcell.org/cgi/doi/10.1105/tpc.107.053256

was able to interact with itself (e.g., dimerize), with three of the five At SCAR or SCAR-like proteins, with the four At ABIs, with ARP3, and with ARPC3, confirming tight interaction inside and between the two complexes. Two recent studies investigated more specifically the role of the At BRK1/HSPC300 subunit in *Arabidopsis* (Djakovic et al., 2006; Le et al., 2006). Both reports showed that defects in BRK1 led to similar overall phenotypes but also demonstrated a drastic reduction in the accumulation of SCAR1 (Djakovic et al., 2006) or SCAR2 (Le et al., 2006). They proposed that the role of BRK1, a component of the Wave/SCAR complex, was to stabilize/protect the SCAR protein, similar to the results described above for the other SCAR-associated proteins in *Drosophila melanogaster* (Kunda et al., 2003; Rogers et al., 2003) and *Dictyostelium discoideum* (Blagg et al., 2003). Although in vivo distribution of these proteins might give further clues as to their role in tip growth and interaction with Arp2/3, their localization within plant cells is not known.

We have approached the problem using haploid protonemal filaments of the moss *Physcomitrella patens*. Growth of this tissue is maintained through cell division and elongation in only the apical cell of the filament (Menand et al., 2007a) and not in the subtending cells. Furthermore, the orientation of cross walls in the two cell types of protonemal filaments is different; cross walls of chloronemal cells are perpendicular, while those of caulonemal are oblique. Also, when filaments are given an orienting vector, such as light or gravity, only the apical cell responds to such gradients by orienting polar tip growth relative to the signal (Cove et al., 1996; Cove and Quatrano, 2004). Hence, in the entire signaling pathway, from perception of the orienting vector to directional tip growth, both elongation and division is confined to a single apical cell (Cove et al., 2006; Menand et al., 2007a). Finally, the tools available in this system (Quatrano et al., 2007), including transformation, gene targeting (Schaefer, 2001; Kamisugi et al., 2005), RNA interference (RNAi) (Bezanilla et al., 2003, 2005) and a fully assembled genome (www.mossgenome.org), will enable us to more easily determine the localization and possible role of the members of these complexes that regulate actin assembly in coupling tip growth with the orientation and deposition of cross walls within a single apical cell.

Previously, we used targeted gene deletion and replacement in *P. patens* to test whether members of protein Arp2/3 play a role in these processes. Similar to the mutants in *Arabidopsis* and maize, gene deletion, or RNAi inhibition of transcripts in *P. patens* for the Arp2/3 subunits ARPC4 (Perroud and Quatrano, 2006), ARPC1 (Harries et al., 2005), and ARP3 (Finka et al., 2007), gave viable mutant phenotypes. However, unlike the phenotypes in *Arabidopsis* and maize, where there are little or no effects in the tip growing cells, such as root hairs or pollen tubes, these mutants in *P. patens* showed a major defect in the tip growth of protonemal filaments. Reduced transcripts of ARPC1 by RNAi prevented polar filament extension upon regeneration of protoplasts as well as for the formation of the leafy shoots or gametophores (Harries et al., 2005). $\Delta arpc4$, on the other hand, developed into gametophores but showed severely restricted tip growth of the protonemal filaments. ARPC4 was localized to the tip of the apical cell in wild-type filaments, the site of the defect in $\Delta arpc4$. Finally, when ARP3 is deleted (Finka et al., 2007), protonemal elongation is inhibited and, concomitantly, the

actin-specific pattern detected with green fluorescent protein (GFP)-talin is abolished in the tip cell.

This study represents a start toward understanding the role of one member of the Wave/SCAR complex, BRK1. We report here the function of BRK1 in apical cells of *P. patens* and its interaction with cell tip-localized members of the Arp2/3 complex as well as with proteins known to be associated with the directional flow of vesicles to cortical sites (e.g., RAB and ROP/RIC proteins) (Mathur, 2005; Smith and Oppenheimer, 2005), more specifically a Rab GTPase that accumulates at the site of tip growth in seed plants (Preuss et al., 2004; de Graaf et al., 2005). We generated a true null ($\Delta brk1$) by targeted gene deletion that led to a dramatic reduction of filament growth, not unlike the phenotypes disrupting the function of members of the Arp2/3 complex. However, cells in $\Delta brk1$ were smaller, divided less frequently, and possessed a pattern of cross walls that were different from the wild type and from the mutant phenotypes of the Arp2/3 complex. Using an inducible GFP-talin to detect actin in living tissue, a characteristic broad accumulation of actin was observed at the tip of wild-type apical cells, whereas in $\Delta brk1$, smaller, more distinct foci of actin were present. Subsequent transformation of $\Delta brk1$ using a yellow fluorescent protein (YFP)-tagged Pp *brk1* gene fully complemented the deletion and localized BRK1 at the tip of the apical cell. Finally, using YFP-tagged lines of ARPC4, BRK1, and At RABA4d, we showed their localization patterns in the absence of each other as well as their role in polar cell growth of the apical cell. Although gametophores were stunted in $\Delta brk1$, they had a normal and characteristic shape, similar to the phenotype in $\Delta arpc4$ (Perroud and Quatrano, 2006). These and other results suggest that BRK1 functions directly or indirectly in the accumulation/stabilization of actin and other proteins required for polar growth in apical cells of filaments but not for the basic structure of the gametophore.

RESULTS

We identified the Pp *brk1* sequence by searching a publicly available *P. patens* sequence database (<http://moss.nibb.ac.jp/>) with the maize Zm *brk1* sequence. The 837-bp EST clone contained the full coding sequence (237 bp) of a close homolog to the original maize protein (see Supplemental Figure 1 online). Using RT-PCR primers designed on the EST clone, we confirmed the presence of transcripts in all vegetative tissue of *P. patens* (see Supplemental Figure 2 online). Sequence similarity with other plant proteins is high (e.g., 62% identity with Zm *brk1*) but significantly lower with non-plant genes (e.g., 38% with *Homo sapiens* HSPC300). The position of the single intron in the genomic sequence (position 1070 of 3316 bp, gPp *brk1*) appeared to be conserved between angiosperms (i.e., maize, rice, and *Arabidopsis*) and *P. patens*. Interestingly, we found a BRK1 homolog in the filamentous brown alga *Ectocarpus siliculosus* (see Supplemental Figure 1 online), but we were unable to identify BRK1 in the single-cell alga *Chlamydomonas reinhardtii*.

Deletion of Pp Brk1

We deleted the full open reading frame (ORF) of *brk1* ($\Delta brk1$), and the single-copy, single-locus transformants (see Supplemental

Figure 3 online) were isolated and all exhibited a uniform phenotype. Compared with the wild type, $\Delta brk1$ protonemal filaments exhibited a dramatic reduction in size as a result of absence of apical cell extension, resulting in very small colonies (Figures 1A to 1D), similar to the phenotypes for mutants in the Arp2/3 complex in *P. patens* (Harries et al., 2005; Perroud and Quatrano, 2006). Lateral branching was reduced or absent in long filament-

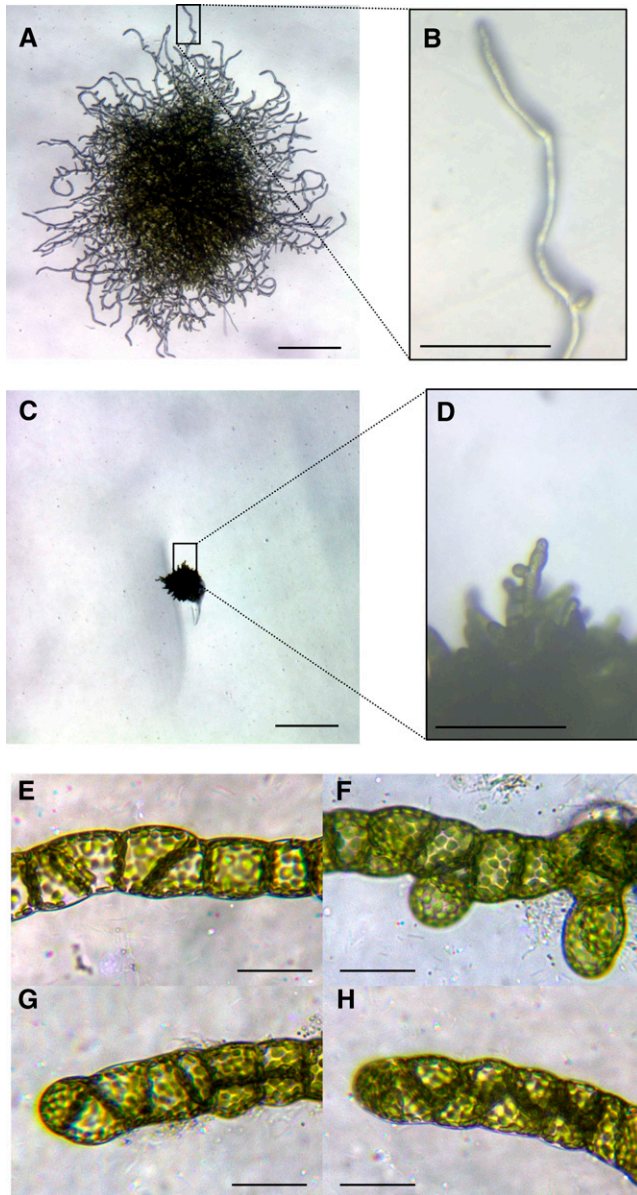


Figure 1. Phenotype of $\Delta brk1$ Shows Lack of Extension Growth of the Apical Cell, Small Colonies, and Cells with Abnormal Planes of Division.

(A) to (D) Protonemal phenotypes of 24-d-old colonies ((A) and (C)) and filaments ((B) and (D)) derived from protoplasts of the wild type ((A) and (B)) and $\Delta brk1$ ((C) and (D)). Bars = 1 mm.

(E) to (H) Protonemal cells of 7-d-old filaments in $\Delta brk1$ derived from tissue fragments. Bars = 50 μ m.

tous stretches (Figures 1E to 1H; see Supplemental Figure 4 online). Cell size measurement confirmed that the main characteristic of the $\Delta brk1$ phenotype is a dramatic reduction in the cell length of protonemal cells (Figure 2A). The average cell length/width ratio in $\Delta brk1$ cells is 0.9, dramatically reduced from the 12.9 and 3.6 ratios found in wild-type caulonemal and chloronemal cells, respectively. But cell size is not the only component responsible for reduced filament length. Filaments arising from regenerating protoplasts of $\Delta brk1$ and the wild type revealed a significant difference in cell number after 4 d. $\Delta brk1$ regenerating filaments contained an average of $3.55 \text{ SD} \pm 1.20$ ($n = 226$) cells compared with $5.85 \text{ SD} \pm 2.84$ ($n = 231$) in the wild type, indicating that cell division is slowed in the mutant protonema (Figure 2B). Hence, the protonema in $\Delta brk1$ displayed an abnormal phenotype compared with the wild type and different from those observed in Arp2/3 mutants in *P. patens* (Harries et al., 2005; Perroud and Quatrano, 2006).

Although cell division continued, the characteristic pattern of cross walls found in wild-type chloronemal and caulonemal cells was absent (Figures 1E and 1F). Auxin treatment, which in the wild type leads to enhanced cell elongation and a caulonema-dominated filamentous network (Ashton et al., 1979), was without detectable effect on $\Delta brk1$. Rhizoids in $\Delta brk1$ were initiated from the gametophore, but like protonemal filaments, they do not undergo tip growth (data not shown). Although the phenotype of $\Delta brk1$ in filaments and colonies was dramatic, the effect on gametophore development was less severe, resulting in a normally shaped gametophore significantly stunted in height (Figure 3) compared with the wild type. No further characterization of the gametophore was undertaken in this study.

To evaluate the impact of deleting BRK1 on the actin cytoskeleton, we isolated $\Delta brk1$ in a line of *P. patens* (HGT-1) that expresses GFP-talin under an inducible heat shock promoter (Finka et al., 2007). Morphologically, HGT-1/ $\Delta brk1$ is identical to $\Delta brk1$ described above, and no GFP signal was detected in the absence of the inducing heat shock. A drastic alteration of the tip accumulation of GFP-talin is observed in the absence of BRK1. In HGT-1 (Figures 4A to 4D), a strong signal is detected, capping the growing tip of the apical cell showing the characteristic actin localization pattern in a tip-growing cell. By contrast, this broad, strong accumulation of an actin cap in HGT-1 is absent in HGT-1/ $\Delta brk1$ (Figures 4E to 4H) where GFP-talin shows a punctate pattern of one to several foci. This pattern of weak, one to several foci of actin localization was observed in many cells and is a consistent difference between HGT-1/ $\Delta brk1$ and HGT-1. Interestingly, the cortical actin filaments observed in HGT-1 (Finka et al., 2007) are maintained in HGT-1/ $\Delta brk1$ (Figures 4A and 4E, respectively), indicating that formation of actin filaments per se is not dependent on the presence of BRK1 but rather that BRK1 is necessary for the proper accumulation of actin at the apical cell tip that leads to cell elongation.

Complementation of $\Delta brk1$ and Localization of BRK1

We transformed $\Delta brk1$ with a vector containing the same targeting sequence as the deletion construct, with the full Pp *brk1* wild-type ORF and the 3xeYFP sequence added at the 3' end. Given the dramatic morphological differences between the wild

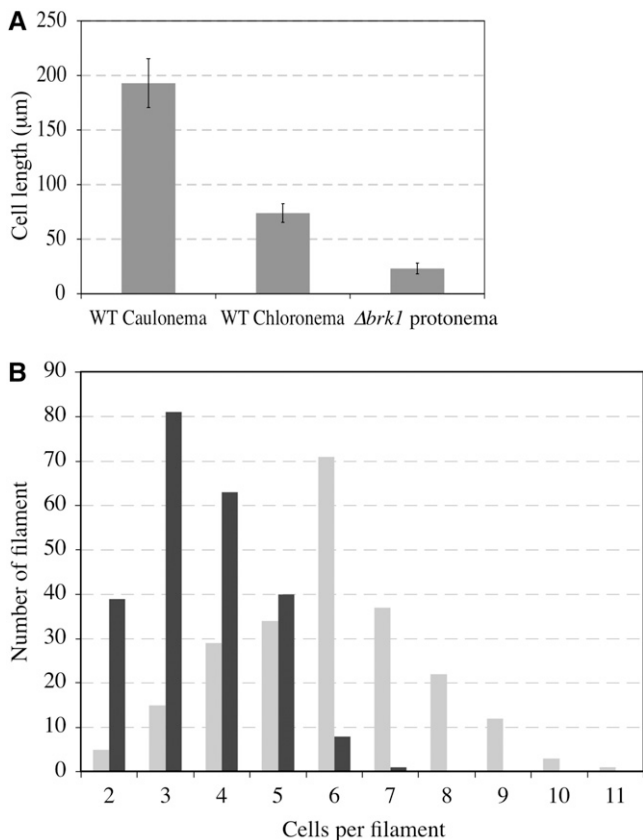


Figure 2. The $\Delta brk1$ Small Phenotype Results from Reduction in Cell Size and Number.

(A) Values represent average cell lengths in micrometers measured on the first three subapical cells of wild-type caulonema and chloronema and $\Delta brk1$ protonema cells. Mean \pm SD ($n \geq 200$ cell for each cell type). **(B)** Repartition of cell number in 4-d-old regenerating filament. Black columns, $\Delta brk1$; gray columns, wild type.

type and $\Delta brk1$, we easily identified transformants that complemented the mutant phenotype. DNA gel blot analysis (see Supplemental Figure 5 online) showing a single copy at the correct insertion site permitted the selection of the strain *brk1-yfp*. Compared with $\Delta brk1$ (see Supplemental Figure 4B online), *brk1-yfp* appeared morphologically normal (see Supplemental Figure 4C online), indicating that BRK1-YFP complemented the mutant phenotype. In addition, the YFP signal was exclusively localized as a cap around the tip of the apical cell (Figure 5) at the site of tip growth.

To determine if the highly similar *At BRK1* could substitute for *Pp brk1*, we transformed $\Delta brk1$ with *At BRK1*, and plants resembling the wild type were screened for a single-copy insertion of the vector (see Supplemental Figure 5 online). We isolated the $\Delta brk1$ -*AtBRK1* line (see Supplemental Figure 4D online) that exhibited a wild-type phenotype (caulonemal and chloronemal cells were clearly differentiated, and buds/gametophores had the characteristic shape and size), indicating that the *Arabidopsis* gene functionally complemented $\Delta brk1$ when expressed at the same genomic position as *Pp brk1*. In addition, RT-PCR ampli-

fication using primers designed on the 5' and 3' untranslated regions of *Pp Brk1* transcript (see Supplemental Figure 6B online) detected a product of the proper spliced size (see Supplemental Figure 6C online). Subsequent sequencing of the $\Delta brk1$ -*AtBRK1* transcript confirmed its hybrid nature: 3' and 5' untranslated regions of moss origin and ORF sequence from *Arabidopsis*. This observation underscored the capacity of *P. patens* to properly splice a gene (*At BRK1*) from a seed plant.

Interaction between Arp2/3 and Wave/SCAR Complexes

We isolated two tagged strains representing each complex, *brk1-yfp* (Wave/SCAR complex) and *yfp-arpc4* (Arp2/3 complex) (Perroud and Quatrano, 2006). For controls, deletion of BRK1 in a *yfp-arpc4* background showed the same phenotype as described above (Figure 1), while deletion of ARPC4 in the *brk1-yfp* background showed the same mutant phenotype as previously described (Perroud and Quatrano, 2006). In both cases, the phenotype was similar (i.e., reduced elongation from the apical cell). Furthermore, using an antibody to GFP, we detected by protein gel blot analysis BRK1-YFP and YFP-ARPC4 in *brk1-yfp* and *yfp-arpc4* and their corresponding deletions (Figure 6A).

As in *brk1-yfp* (Figures 6B to 6D), BRK1-YFP remained localized in the apical tip cell of $\Delta arpc4$ (Figures 6E to 6G), indicating that BRK1 localization was not dependent on the presence of ARPC4. However, no YFP-ARPC4, localized at the cell tip in *yfp-arpc4* (Figures 6H to 6J), signal was localized in the apical tip cell of $\Delta brk1$ (Figures 6K to 6M). These results clearly indicated that BRK1, of the Wave/SCAR complex, was necessary for the proper localization of ARPC4 of the Arp2/3 complex.

To further assess the effect of $\Delta BRK1$ on cell tip elongation, we deleted *brk1* in the *YFP-AtRabA4d* background. In this strain, *YFP-AtRABA4d* protein accumulates specifically at the tip of elongating cells. Furthermore, the signal is very strongly correlated with the rate of tip growth: strong expression in the longer caulonemal cells (Figures 7A to 7C) but weak expression in the shorter chloronemal cell (Figures 7D to 7F). Since extension tip

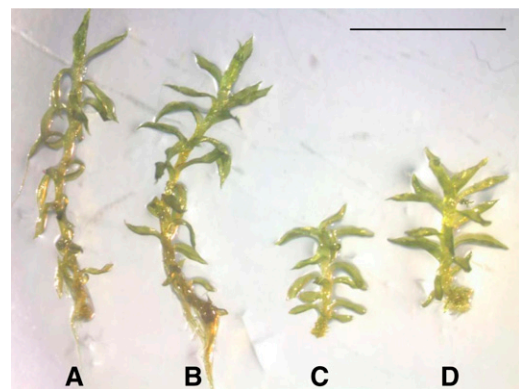


Figure 3. The phenotype of $\Delta brk1$ Presents Normally Shaped but Stunted Gametophores.

Wild type (**[A]** and **[B]**) and $\Delta brk1$ (**[C]** and **[D]**) gametophores. Bar = 0.5 cm.

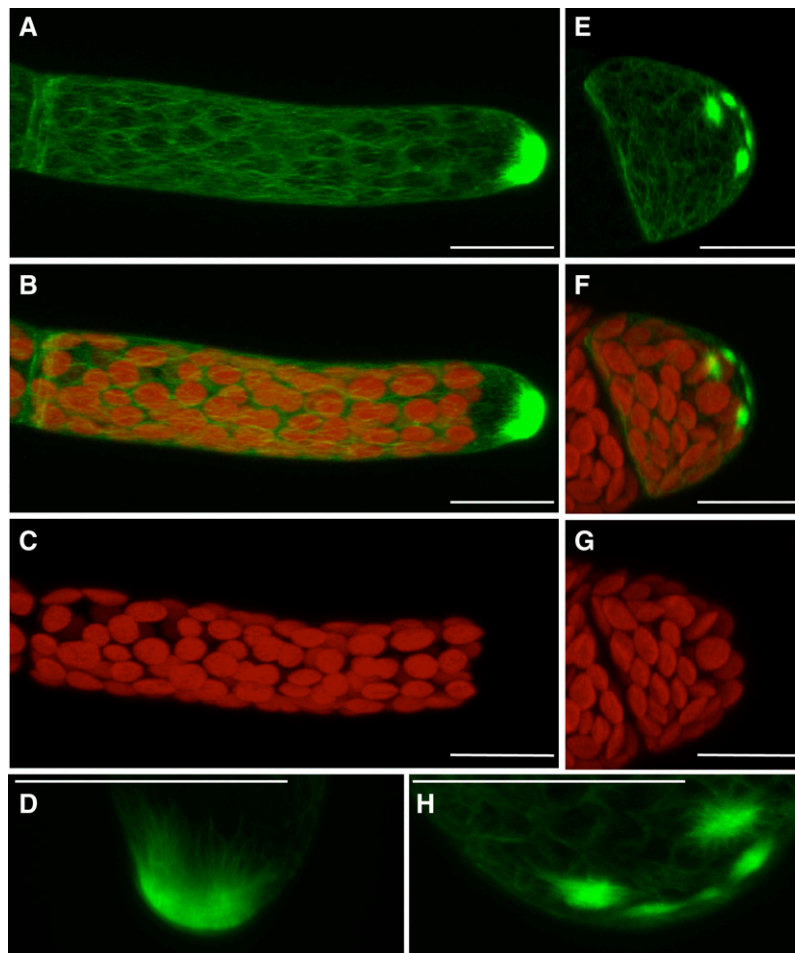


Figure 4. Effect of $\Delta brk1$ on GFP-Talin Labeling in a Tip Cell.

GFP-talin labeling observed in induced HGT-1 and $\Delta brk1$ in the HGT1 background. Bars = 20 μm .

(A) to (D) HGT-1.

(E) to (H) $\Delta brk1$ in HGT-1 background.

(A), (D), (E), and (H) Green signal only,

(B) and (F) Green and red signals (detecting chloroplasts) merged.

(C) and (G) Red signal only.

(D) and (H) Higher magnifications of (A) and (E), respectively.

growth is reduced or absent when members of the Arp2/3 and Wave/SCAR complexes are eliminated or reduced (Harries et al., 2005; Perroud and Quatrano, 2006), we asked whether *YFP-AtRABA4d* is localized in tip cells in $\Delta arpc4$ and in $\Delta brk1$. In both deletion lines, we observed a loss of tip accumulation of *YFP-AtRABA4d* (Figures 7G to 7L). Interestingly, protein gel blot analysis (see Supplemental Figure 7 online) confirmed again that *YFP-AtRABA4d* is still present in the cell, indicating that the absence of BRK1 and ARPC4 is necessary for the tip localization of *YFP-AtRABA4d* but not its accumulation.

DISCUSSION

The major mutant phenotype of $\Delta brk1$ appears to be confined primarily to the filamentous stage (i.e., severe reduction in apical

cell growth and abnormal positioning of cross walls). The disappearance of the long, narrow cell type, the formation of unique cubical shaped cells, and the absence of a typical apical cell accompany this lack of apical cell growth in $\Delta brk1$. In addition, the appearance of $\Delta brk1$ filaments is clearly very different from filaments of wild-type and published mutants of the Arp2/3 complex (i.e., ARPC1 [Harries et al., 2005] and ARPC4 [Perroud and Quatrano, 2006]), especially with respect to the random positioning of the cross walls and the rate of cell division. Despite these striking differences, $\Delta brk1$ maintains a viable filamentous colony that ultimately develops into normally shaped but stunted gametophores. Whether the developmental pattern of bud initiation and gametophore formation in $\Delta brk1$ is similar to the wild type was not investigated in this study. Hence, the relatively simple morphology of *P. patens* and the single apical cell allows

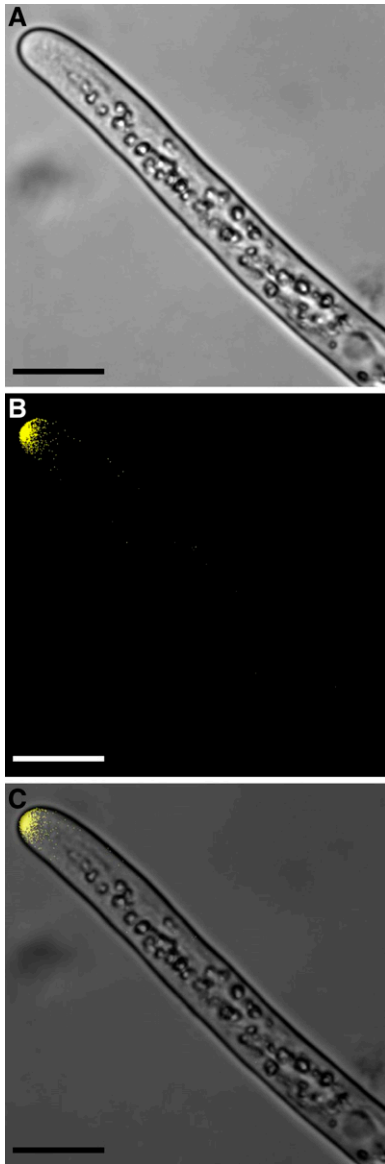


Figure 5. BRK1 Is Localized at the Tip of the Extension Site of the Apical Cell.

Caulonemal apical cells from *brk1-yfp* in white light (**A**), the same cell viewed for the YFP signal under fluorescence (**B**), and the merged images (**C**). Bars = 20 μ m.

one to clearly see the effect of the loss of BRK1 that is likely to be masked in more complex tissue interactions and redundant regulatory networks of more complex developmental patterns.

Using an inducible promoter to visualize actin during apical cell growth in wild-type cells, we confirmed the results of Finka et al. (2007), who showed that an actin cap is strongly and clearly localized in the dome of a normal apical cell, with a filamentous network in other areas of the apical cell. All other protonemal cells show the filamentous network of actin but lacked the accumulation of actin observed in the apical cell. Vidali et al.

(2007) recently observed actin in fixed apical cells of *P. patens* using a rhodamine phalloidin staining procedure. They showed a filamentous network of actin in the cytoplasm, the same as our results and those of Finka et al. (2007). However, the staining of actin at the tip of the apical cell with rhodamine phalloidin showed a clear difference compared with the *in vivo* localization of GFP-talin used in this work and the publication of Finka et al. (2007) (i.e., the most apical area lacked any actin staining with rhodamine phalloidin). Vidali et al. (2007) did observe, however, a longitudinally oriented, cable-like actin structure in the subapical zone. The observed differences may be due to the fact that we used an inducible promoter to express GFP-talin to visualize actin in living tissue compared with actin in fixed tissue (Vidali et al., 2007). Perhaps the actin accumulation at the tip of a growing filament is not preserved or becomes rearranged in fixed material. Alternatively, our observations may be explained by the differences in the interactions between talin and phalloidin with actin filaments.

In $\Delta brk1$, the pattern of actin localization is significantly different from the wild type, indicating that removal of one component of the Wave/SCAR complex results in a noticeable alteration in actin formation/distribution. Although the accumulation of actin is dramatically reduced at the tip, it is not eliminated; rather, it is concentrated in one or more small foci. Interestingly, the cortical actin filaments observed in HGT-1 (Finka et al., 2007) and the filamentous network we observed in the cytoplasm remain in HGT-1/ $\Delta brk1$ in the absence of the large accumulation of actin at the apical cell tip. We believe that BRK1, and perhaps the entire Wave/SCAR complex, may play a selective role in forming or maintaining the subset of actin that leads to localization of specific proteins required for cell elongation (e.g., ARPC4 and At RABA4d) to the tip of the apical cell.

We also show that BRK1-YFP is clearly localized only in the tip of the apical cell, at the exclusive site where growth and cell division occur and where actin accumulates. By being able to insert the *brk1-yfp* sequences into the deleted site by homologous recombination, we were not only able to follow the *in vivo* localization of BRK1 using its own promoter but to show that BRK1-YFP complemented the mutant phenotype. Hence, the *in vivo* localization of BRK1 and mutant phenotype indicates a likely role in apical tip growth. A similar *in vivo* tip localization and reduction of cell extension was reported in *P. patens* when ARPC4 of the Arp2/3 complex was deleted (Perroud and Quatrano, 2006). Interestingly, the tip localization is similar to that of actin as discussed above. The reduction in apical cell growth indicates that ARPC4 and BRK1, and possibly the Arp2/3 and SCAR complexes, are both likely to be part of the mechanism for apical cell growth in *P. patens*, which requires the accumulation of actin. Is there any similarity between these results and other tip-growing cells in vascular plants?

A recent study by Menand et al. (2007b) showed in *Arabidopsis* that the basic helix-loop-helix transcription factors At RHD6 and At RSL1 are specifically required for the development of root hairs. They also showed that expression of RSL1 from *P. patens* (Pp RSL1), under the cauliflower mosaic virus 35S promoter, in the At *rhd6-3* mutant resulted in the formation of wild-type root hairs. Thus, the Pp *rsl1* gene from *P. patens* can substitute for loss of At RHD6 function in *Arabidopsis*. Interestingly, in

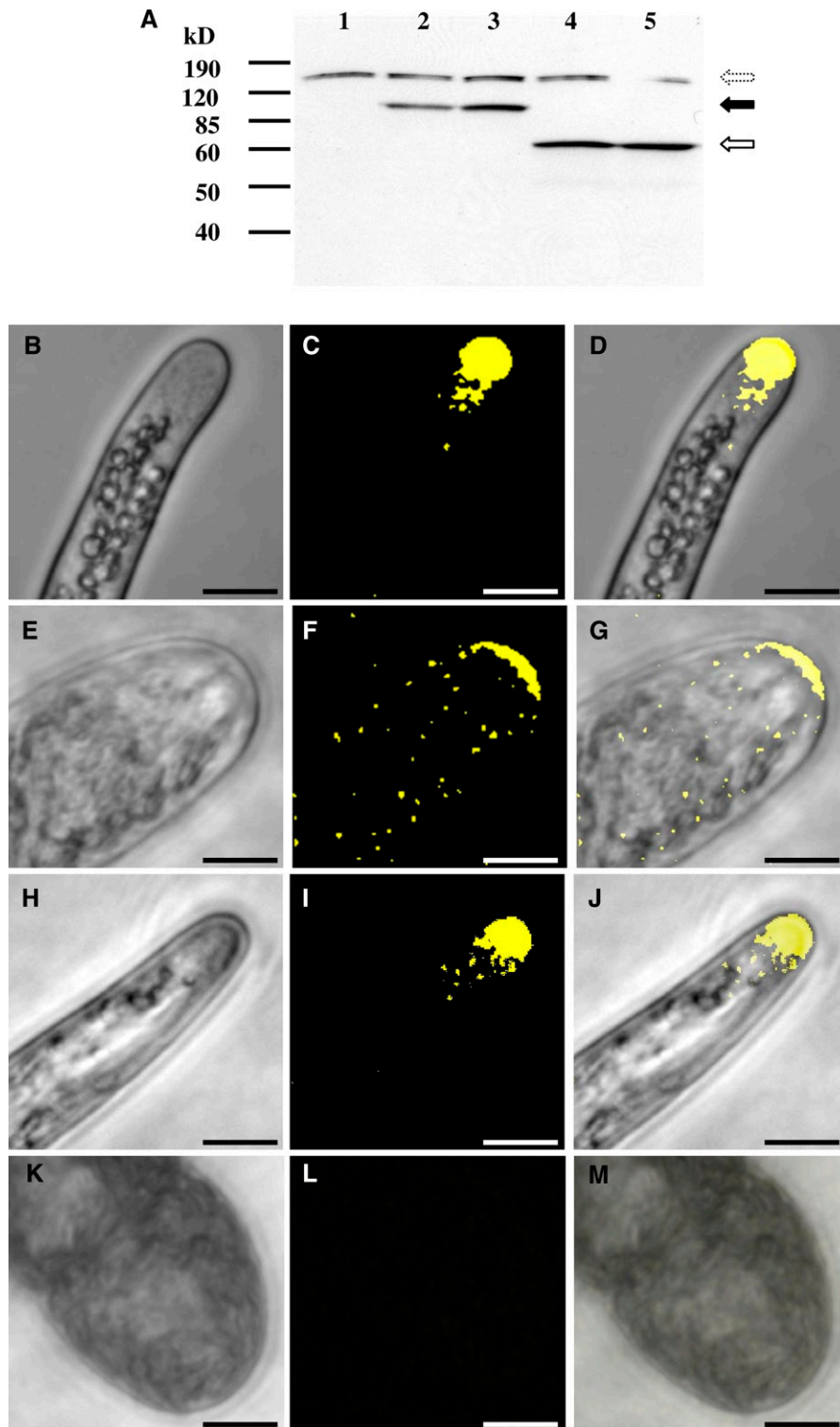


Figure 6. ARPC4 Is Expressed in the Absence of BRK1 but Fails to Localize to the Apical Tip.

(A) Immunoblots using GFP antibody were performed on soluble extracts from the wild type (lane 1), *brk1-yfp* (lane 2), $\Delta arpc4$ in *brk1-yfp* (lane 3), *yfp-arpc4* (lane 4), and $\Delta brk1$ in *yfp-arpc4* (lane 5). Dashed arrow identifies a nonspecific epitope detected by the GFP antibody, a black arrow shows BRK1-YFP, and an open arrow shows YFP-ARPC4. The observed molecular masses of these fusion proteins correspond well to the predicted ones: ~60 to 65 kD for YFP-ARPC4 (2xYFP + ARPC4, predicted 70 kD) and ~80 to 85 kD for BRK1-YFP (3xYFP + BRK1 predicted 83 kD).

(B) to (M) White light (left column), fluorescence (middle column), and merged (right column) images of caulonema tip cells. *brk1-yfp* (**[B]** to **[D]**), $\Delta arpc4$ in *brk1-yfp* (**[E]** to **[G]**), *yfp-arpc4* (**[H]** to **[J]**), and $\Delta brk1$ in *yfp-arpc4* (**[K]** to **[M]**). Bars = 10 μ m.

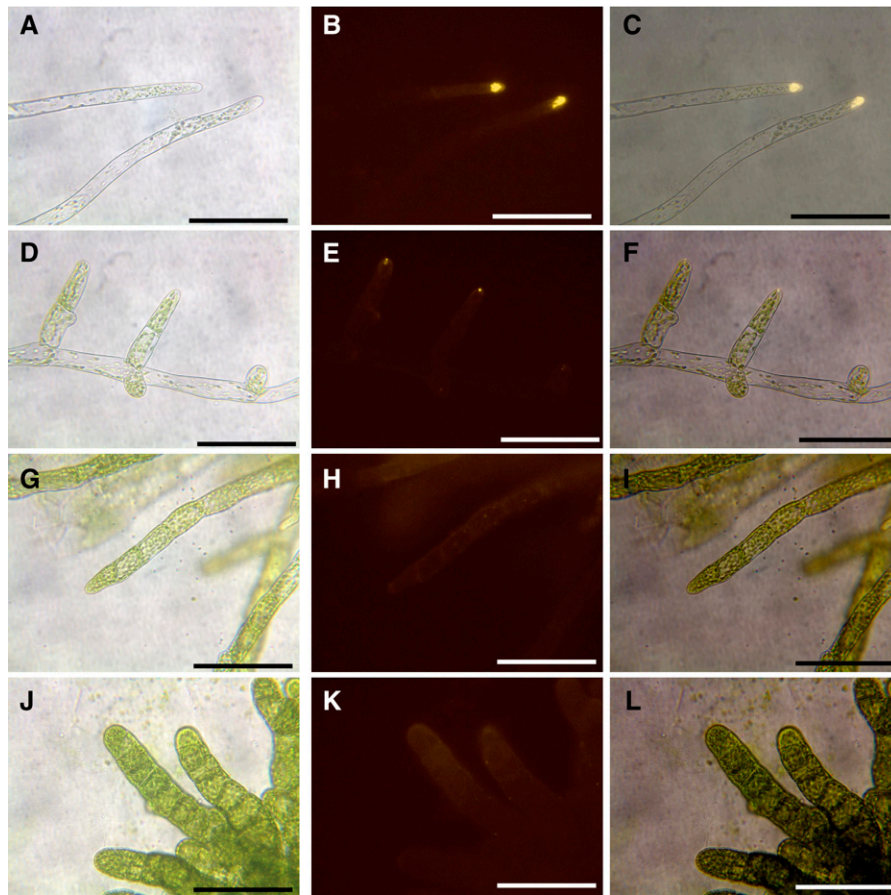


Figure 7. $\Delta brk1$ and $\Delta arpc4$ in YFP-AtRABA4d-Tagged Background.

White light (left column), fluorescence (middle column), and merged (right column) images of protonema tip cells. Bars = 100 μm .

(A) to (C) YFP-AtRABA4d signal in caulonema cells.

(D) to (F) YFP-AtRABA4d signal in chloronema cell.

(G) to (I) $\Delta arpc4$ in YFP-AtRabA4d background.

(J) to (L) $\Delta brk1$ in YFP-AtRabA4d background.

P. patens, the *Pp rs1/1 Pp rs2/2* double mutant does not form caulonemal cells, and the protonema of this mutant consists of chloronemal cells only. The *Pp rs1/1 Pp rs2/2* double mutants have normal gametophores but possess only a few, very short rhizoids. No other defective phenotypes were detected in the sporophyte in the single or double mutants. Several of these phenotypes in protonemal filaments are similar to $\Delta brk1$ (e.g., reduced colony growth, lack of caulonemal cells and rhizoids, and normal gametophores). However, overall growth reduction is more severe in $\Delta brk1$, and distinct differentiation of either of the protonemal cell types is lacking. Although it is clear that *Pp RSL1* and *Pp RSL2* together regulate the development of caulonemal cells and rhizoids, but not chloronemal cells, the role of BRK1 in the moss gametophyte appears to be more central to overall apical cell growth.

If BRK1 is important for cells to undergo proper polar tip growth, one would expect mutations in *At BRK1* to show aberrant cellular phenotypes in similar tip-growing cells of *Arabidop-*

sis (i.e., root hairs and pollen tubes). Although the effects on the single-cell extensions of leaf epidermal cells (i.e., trichomes) are affected, little or no observable phenotypes are found in *Arabidopsis* root hairs and pollen tubes (Djakovic et al., 2006). Even in the numerous T-DNA insertional mutants of members of the Arp2/3 complex (for review, see Deeks and Hussey, 2005; Szymanski, 2005), only a weak effect on tip growth of root hairs has been reported (Mathur et al., 2003; Li et al., 2004). One possibility is that tip growth in root hairs and pollen tubes occurs by a different mechanism than apical cell growth and division in *P. patens* filaments. Interestingly, Menand et al. (2007b) showed in *Arabidopsis* that the basic helix-loop-helix transcription factors *At RHD6* and *At RSL1* are specifically required for the development of root hairs but are not essential for pollen tube growth. Perhaps in seed plants, BRK1 may normally support tip growth but when inactivated another compensating protein(s)/ pathway(s) becomes engaged and replaces BRK1 function. Menand et al. (2007b) concluded that the molecular function of

Pp RSL1 and At RHD6 has been conserved since the divergence of seed plants and suggests that the same molecular mechanism controls the development of *Arabidopsis* root hairs and *P. patens* caulonema and rhizoids.

With respect to At *BRK1*, however, we showed in this study that this gene restored tip growth in $\Delta brk1$. This result demonstrated that At *BRK1* is fully capable of functioning in apical cell growth and cell division of *P. patens* filaments, even though a mutation in this gene did not result in loss of tip growth in these cells in *Arabidopsis*. However, we have not determined if Pp *brk1* can complement the *Arabidopsis* T-DNA mutant.

To begin to understand the interaction between ARPC4 and BRK1 in relation to apical cell growth and the role they play in directing macromolecules other than members of these complexes to the site of cell extension, we followed the localization of both ARPC4 and BRK1 as well as At RABA4d (a Rab11-like GTPase). We show in our study that At RABA4d-YFP is localized in apical cells of *P. patens* filaments similar to the report localizing Rab11 GTPase at the tip of the elongating pollen tube. This Rab11 GTPase is essential for growth and directed membrane trafficking to the elongating tip of tobacco (*Nicotiana tabacum*) pollen tubes (de Graaf et al., 2005). In *P. patens*, At RABA4d appears to be a functionally relevant marker for tip growth (i.e., its level of accumulation at the apical cell tip is proportional to the rate of elongation, with less accumulating at the tip of chloronemal cells than in the more rapidly elongating caulonemal cells) (cf Figures 7A to 7C [caulonemal] with 7D to [chloronemal]).

At RABA4d is not localized in $\Delta brk1$ or in $\Delta arp4$, indicating that BRK1 and ARPC4 are essential for the localization of proteins directly or indirectly associated with vesicle targeting that are not part of the Arp2/3 or SCAR complexes per se. However, localization of BRK1 itself is not sufficient for extension of the apical cell, since without ARPC4, no apical cell growth occurs even though BRK1 is properly localized. BRK1 is required for ARPC4 and actin to accumulate at the tip of the apical cell. Since apical cell growth was absent in both deletion lines (i.e., $\Delta brk1$ and $\Delta arp4$), our working hypothesis is that accumulation of ARPC4 of the Arp2/3 complex and actin are the active components for tip growth. One hypothesis is that BRK1 appears to serve in part to localize/stabilize the Arp2/3 complex, actin, and At RABA4d to the tip of the apical cell where they direct in concert apical cell growth. Since $\Delta brk1$ has a distinct set of cellular phenotypes not seen in $\Delta arp4$, BRK1 may also serve to localize/stabilize other complexes or proteins essential for apical cell growth.

Is the role of BRK1 to localize apical cell proteins directly or indirectly? The latter hypothesis is supported by the observation that in $\Delta arp4$, At RABA4d is not localized, suggesting that the lack of At RABA4d localization in $\Delta brk1$ may be due to the interaction of BRK1 with the Arp2/3 complex or with actin itself and/or some other component(s). Since BRK1 still accumulates at the tip of apical cells in $\Delta arp4$ (which has reduced growth), BRK1 localization itself is not sufficient for apical cell growth or for the localization of At RABA4d. Also, the abnormal pattern of actin in $\Delta brk1$ apical cells is probably not due to the localized presence of the Arp2/3 complex since we show that ARPC4 is not localized at the apical cell tip in the absence of BRK1. Hence, our more refined hypothesis is that the localization of ARPC4

(Arp2/3) is required for proper tip growth, while BRK1 itself is not required but serves to stabilize the Arp2/3 complex (if present), the SCAR protein (Lee et al., 2005; Djakovic et al., 2006), the actin cytoskeleton, and other apical cell-localized proteins (e.g., RABA4d) either directly or through Arp2/3 or another complex.

METHODS

Plant Material, Culture Conditions, and Treatments

Physcomitrella patens (Gransden) tissue (wild type) was routinely grown on cellophane disks overlaying 0.7% agar (Plant Cell Culture Agar; Sigma-Aldrich) in Petri dishes (9 cm) containing minimal medium plus 0.5 g/L (di)ammonium tartrate (Ashton and Cove, 1977). These cultures were grown at 25°C under a long-day light cycle (16 h light [80 $\mu\text{mol m}^{-2} \text{s}^{-1}$]/8 h dark). Zeocin (Invitrogen) was added at 100 $\mu\text{g/L}$ to the media to select for antibiotic-resistant cells. Phenotypic analyses were completed on minimal media without addition of (di)ammonium tartrate. Cell measurements were performed on three first subapical cells of 7-d-old protonema stained with calcofluor (Sigma-Aldrich). To visualize actin in living cells, we used the HGT-1 strain that expresses GFP-talin under an inducible heat shock promoter as described by Finka et al. (2007). Briefly, a cellophane disk covered with a 6-d-old culture was transferred to a preheated Petri dish containing appropriate medium and incubated for 1 h at 37°C. Cellophane was then transferred back to a Petri dish and placed in regular growth conditions. Observations were performed 10 to 15 h after treatment.

Protoplasts were produced according to Ashton et al. (2000) with slight modifications. Shortly, 1-week-old protonema were treated with 0.5% driselase in 8.5% mannitol for 45 min, passed through a 100- μm sieve, incubated for 15 min, and passed through a 50- μm sieve. The protoplasts of the final flow-through, washed twice in 8.5% mannitol, were ready for further use. Cell count on filaments was performed on 4-d-old regenerated protoplasts plated at 15×10^3 protoplasts per Petri dish (9 cm).

Molecular Procedures

All PCR reactions were performed with Elongase mix (Invitrogen), and all restriction enzymes came from New England BioLabs. All PCR fragment clonings were performed using pTopo2.1 (Invitrogen). *P. patens* genomic DNA and total mRNA were routinely isolated from a 1-week-old culture using the Nucleon Phytopure Plant DNA extraction kit (GE Healthcare) and the RNeasy plant mini kit (Qiagen). Confirmation of transcripts for the EST AW738961.1 coding for Pp *Brk1* was performed using the primers P1 (5'-AACGGACGTCGCAGGTGT-3') and P2 (5'-GTTGAATCAAATGCTCAAG-3') on cDNA synthesized on wild-type mRNA using the ThermoScript RT-PCR system kit (Invitrogen). The sequence obtained perfectly matched the EST.

A partial genomic sequence of Pp *Brk1* was determined by PCR using the same primers P1 and P2 on *P. patens* genomic DNA. Inverse PCR (IPCR) was then performed to obtain 5' and 3' genomic sequence. Genomic DNA was treated briefly by the *NdeI* restriction enzyme, religated to itself, and used as a template for two successive PCR reactions using primers designed to amplify either the 5' or 3' flanking sequence of Pp *Brk1* (primers for 5' IPCR: P3, 5'-CCTCGAGATCTGGCTACAAC-3'; P4, 5'-TCCTAGTCTGGGAACACGG-3'; PCR 2, P5, 5'-GCAAAGACGCTAAGTCTCAG-3'; P6, 5'-TCCGACCCACAAGCAATTCC-3'; primers for 3' IPCR: P7, 5'-CCTCAGGATCTTGAATCGCG-3'; P8, 5'-TGACTCCCGGTAGTAGGG-3'; PCR 2; P9, 5'-TCGAGCTCACGGAGTTGAAG-3'; P10, 5'-AGGAGTTCGAAACCCTCAGC-3'). Sequencing and assembly of these new extended 5' and 3' sequences to the core coding region of the locus gave a genomic fragment of 3316 bp that was used as the reference for the rest of this work (gPp *brk1*). DNA gel blot analysis was routinely performed

on wild-type and transgenic plants with 1.0 μg of genomic DNA per digestion. After digestion with specific restriction enzymes, the reactions were resolved on a 0.6% agarose gel and transferred to N-Hybrid (GE Healthcare). Hybridization and detection were performed with the non-radioactive DIG method (Roche Diagnostic). The PCR DIG synthesis kit (Roche Diagnostic) was used to make probes. Following the gene-specific probe hybridization, the membrane was always stripped and tested for the presence of nonspecific plasmid insertion with a probe designed to detect the resistance gene.

Establishment of the *YFP-AtRabA4d* Line

The *YFP-AtRabA4d P. patens* line was obtained by constitutively overexpressing *eYFP-AtRabA4d* cDNA (generous gift of E. Nielsen) under the 35S promoter. This overexpressing cassette was incorporated in a vector containing the hygromycin resistance cassette flanked by the lox site and the 108 genomic locus used as targeting sequence (Schaefer and Zryd, 1997). The final vector was cut with *SwaI* restriction enzyme to linearize the construct prior to transformation. Polyethylene glycol-mediated protoplast transformation was performed according to Schaefer and Zryd (1997). A uniformly labeled colony was then picked, and Cre recombinase treatment (Chakhparonian, 2001) was applied to remove the selective marker. The final line, containing only one 35S:*YFP-AtRabA4d* overexpression copy, was then named *YFP-AtRabA4d* and used as the wild type for further work.

Deletion and Complementation Vector Constructs

The gene deletion vector was designed to remove the full ORF of Pp *Brk1*. The deletion vector was generated by PCR using the primers P11 (5'-TCTAAGAACTGTTTGAAG-3') and P12 (5'-AATCAAGTTCCTGTGGA-3') with the gene deletion construct as template. The resistance cassette *Lox-35S:Zeocin-Noster-Lox* was obtained by transferring the blunted fragment *EcoRI-XbaI* from the vector p35S-Zeo (generous gift of Y. Hiwatashi) into the blunted *BamHI-XbaI* site of the *Lox-35S:hphCamVter-Lox* cassette (generous gift from D.S. Schaefer). The regions 30 to 940 bp (5' of the ORF) and 1643 to 3134 bp (3' of the ORF) of gPp *brk1* were PCR amplified with the addition of the restriction enzyme sites *Sac2* and *SpH1* at each end of the 5' arm and *Sall* and *Nsil* at each end of the 3' arm and cloned using these enzymes on each side of the *Lox-35S:Zeocin-Noster-Lox* cassette. Double crossing-over with this construct would result in the total deletion of the Pp *Brk1* ORF. The tagging vector was constructed with a detectable fluorescent tag to complement the mutant obtained with the full deletion vector and labeled BRK1. It contained the region 30 to 3134 of gPp *brk1* into which the 3Xe*YFP* coding sequence had been inserted at position 1632 (C-terminal of BRK1). This vector did not contain any resistance cassette and required a visual screen to determine if complementation occurred. The complementation vector with the At *BRK1* homolog was built as follows: the *Arabidopsis thaliana* genomic sequence containing the At *BRK1* ORF position 216 to 474 was flanked with the same two moss genomic fragments used in the deletion vector. This vector, as the tagging vector, did not contain any resistance cassette and thus needed a visual screen to determine the complementation effect.

Transformation of *P. patens*

Polyethylene glycol-mediated protoplast transformation was performed according to Schaefer and Zryd (1997). To eliminate any episomal-resistant colonies (Ashton et al., 2000), two rounds of selection were undertaken using the appropriate antibiotic. Resistant colonies were then homogenized and plated in duplicate. After 1 week of growth, one of the two cellophane pads was transferred to a medium containing the antibiotic, while the other pad remained on antibiotic-free medium. After one additional week of growth, any difference in growth of a specific clone of

tissue on these different media resulted in that specific clone being discarded (i.e., a nonintegrated clone). The same procedure and vector were used with the four strains in this study (e.g., wild type, HGT-1, *YFP-arp4*, and *YFP-AtRabA4d*). Transformations with both complementation vectors were performed with plasmid-based vectors linearized with the restriction enzyme *Nsil*. After transformation and regeneration of mutant protoplasts, the screen for transformants was performed visually by looking for wild-type growing colonies in mutant backgrounds.

Protein Analysis

All chemicals were routinely obtained from Sigma-Aldrich. Tissue from 7-d-old culture was harvested and drained of excess water between 3M paper sheets and quickly frozen in liquid nitrogen. Tissue was ground with a mortar and pestle, and ice-cold extraction buffer (100 mM $\text{NaH}_2\text{PO}_4/\text{Na}_2\text{HPO}_4$, 10 mM DTT, 10 mg/mL leupeptin, and 20% glycerol, pH 7) was added at 1:1 (w/v). The extract was homogenized by vortexing and spun for 10 min at 14,000g at 4°C. The supernatant was then transferred to a new tube, and protein concentration was determined by the Bradford assay (Bio-Rad Laboratories). Proteins (80 μg per sample) were separated using a 10% SDS-acrylamide gel and then transferred onto a nitrocellulose membrane (GE Osmonic Labstore). After 1 h in blocking solution (25 mM Tris-HCl, pH 7.5, 100 mM NaCl, and 0.1% Tween 20 [TBS-T] + 2.5% nonfat dry milk), the membrane was incubated overnight with constant shaking in a solution containing monoclonal GFP antibody (BD Biosciences) at 1:10,000. After three washes in TBS-T, the membrane was incubated for 1 h with horseradish peroxidase-conjugated anti-mouse IgG (Jackson Immunochemical Laboratories) in TBS-T at 1:20,000. Detection was finally performed using the ECL method (GE Healthcare).

Sequence Analysis

Routine searching for and comparing of sequences were performed using the National Center for Biotechnology Information (NCBI) sequence software (<http://www.ncbi.nlm.nih.gov/>). Multiple sequence alignments were done using ClustalW software (<http://www.ch.embnet.org/software/ClustalW.html>), while alignment visualization was performed using the Boxshade 3.21 software. Cutoff for identity was set at 50% (black box) and for similarity at 40% (gray box) (http://www.ch.embnet.org/software/BOX_form.html).

Microscopy Observations

All photographs were taken with a Spot RT Slider camera (Diagnostic Instruments) mounted on either an inverted Zeiss microscope or an Olympus dissecting microscope equipped with epifluorescence irradiation. Images were then processed using Image J and Adobe Photoshop software. Confocal microscopy was performed either on a Leica TCS SP2 laser scanning confocal microscope or on a Zeiss LSM 510 META NLO confocal microscope. YFP signal was observed using a laser excitation line at 514 nm and a detection band between 520 and 530 nm, GFP signal was observed with a laser excitation at 488 nm and a detection band between 530 to 550 nm, and the red (chloroplast) signal was observed using a 488-nm laser excitation line and detection band between 700 to 730 nm. Images were then processed using either Bitplane Imaris software or ImageJ 1.37v software. At high magnification, a threshold was used to improve the readability of the signal. Therefore, we only measured the amount of YFP qualitatively and not quantitatively.

Accession Numbers

Sequence data from this article can be found in the GenBank/EMBL data libraries under accession numbers AW738961.1 (EST sequence for Pp

BRK1), DQ522238 (Brk1 genomic locus), and NM_127829 (AT2G22640.1; At BRK1 genomic sequence). Protein sequences used in the alignment of Supplemental Figure 1 online were obtained from NCBI (<http://www.ncbi.nlm.nih.gov/>): *Zea mays* Q8RW98, *Oryza sativa* AK120917, *Arabidopsis* Q94JY4, *Ectocarpus siliculosus* and *Dictyostelium discoideum* EAL67856, *Drosophila melanogaster* NM_166648, *Homo sapiens* AAH07929, and *Xenopus tropicalis* LOC548748.

Supplemental Data

The following materials are available in the online version of this article.

Supplemental Figure 1. BRK1 Proteins from Plants and Other Organisms Are Similar.

Supplemental Figure 2. RT-PCR Analysis of Pp *brk1* Transcripts.

Supplemental Figure 3. DNA Gel Blot Hybridization of Wild-Type, $\Delta brk1$, and *brk1-yfp* Strains.

Supplemental Figure 4. Different Complemented Lines of $\Delta brk1$.

Supplemental Figure 5. DNA Gel Blot Hybridization of Wild-Type, $\Delta brk1$, and $\Delta brk1$ -*Atbrk* Strains.

Supplemental Figure 6. Complementation of $\Delta brk1$ with a Genomic Sequence of At *BRK1* Is Correctly Spliced and Complements the *P. patens* Mutant.

Supplemental Figure 7. Protein Gel Blot Analysis of YFP-AtRABA4d Accumulation in $\Delta brk1$ and $\Delta arp4$.

ACKNOWLEDGMENTS

We thank members of the Quatrano lab for their help, especially Aihong Pan for her excellent technical assistance and David Cove for his expert advice and suggestions. We also acknowledge the valuable assistance of Howard Berg and his microscope facilities at the Donald Danforth Plant Science Center (St. Louis, MO). We thank Erik Nielsen of the Donald Danforth Plant Science Center for sharing unpublished data and for furnishing the eYFP-AtRabA4d cDNA. The vector p35S-Zeo and the Lox35S:hphCamVter-Lox cassette were the generous gifts of Y. Hiwataashi and D.S. Schaefer, respectively. Thanks also to Y. Saidi and A. Finka for providing us with the HGT-1 strain of *P. patens* and for their valuable suggestions with its handling. This research was funded by a grant from the National Science Foundation to R.S.Q. (IBN 0112461).

Received May 30, 2007; revised January 11, 2008; accepted January 25, 2008; published February 8, 2008.

REFERENCES

- Ashton, N.W., Champagne, C.E.M., Weiler, T., and Verkoczy, L.K. (2000). The bryophyte *Physcomitrella patens* replicates extrachromosomal transgenic elements. *New Phytol.* **146**: 391–402.
- Ashton, N.W., and Cove, D.J. (1977). The isolation and preliminary characterization of auxotrophic and analogue resistant mutants in the moss *Physcomitrella patens*. *Mol. Gen. Genet.* **154**: 87–95.
- Ashton, N.W., Grimsley, N.H., and Cove, D.J. (1979). Analysis of gametophytic development in the moss, *Physcomitrella patens*, using auxin and cytokinin resistant mutants. *Planta* **144**: 427–435.
- Basu, D., El-Assal, S.E.D., Le, J., Mallery, E.L., and Szymanski, D.B. (2004). Interchangeable functions of *Arabidopsis* PIROGI and the human WAVE complex subunit SRA1 during leaf epidermal development. *Development* **131**: 4345–4355.
- Basu, D., Le, J., El-Assal, S.E.-D., Huang, S., Zhang, C., Mallery, E.L., Koliantz, G., Staiger, C.J., and Szymanski, D.B. (2005). DISTORTED3/SCAR2 is a putative arabidopsis WAVE complex subunit that activates the Arp2/3 complex and is required for epidermal morphogenesis. *Plant Cell* **17**: 502–524.
- Bezanilla, M., Pan, A., and Quatrano, R.S. (2003). RNA interference in the moss *Physcomitrella patens*. *Plant Physiol.* **133**: 470–474.
- Bezanilla, M., Perroud, P.-F., Pan, A., Klueh, P., and Quatrano, R.S. (2005). An RNAi system in *Physcomitrella patens* with an internal marker for silencing allows for rapid identification of loss of function phenotypes. *Plant Biol.* **7**: 251–257.
- Blagg, S.L., Stewart, M., Sambles, C., and Insall, R.H. (2003). PIR121 regulates pseudopod dynamics and SCAR activity in *Dictyostelium*. *Curr. Biol.* **13**: 1480–1487.
- Chakhparonian, M. (2001). Développement d'Outils de la Mutagenèse Ciblée par Recombinaison Homologue chez *Physcomitrella patens*. PhD dissertation (Lausanne, Switzerland: Université de Lausanne).
- Cove, D., Bezanilla, M., Harries, P., and Quatrano, R. (2006). Mosses as model systems for the study of metabolism and development. *Annu. Rev. Plant Biol.* **57**: 497–520.
- Cove, D., Quatrano, R., and Hartmann, E. (1996). The alignment of the axis of asymmetry in regenerating protoplasts of the moss, *Ceratodon purpureus*, is determined independently of axis polarity. *Development* **122**: 371–379.
- Cove, D.J., and Quatrano, R.S. (2004). The use of mosses for the study of cell polarity. In *New Frontiers of Biology*, A.J. Wood, M.J. Oliver, and D.J. Cove, eds (Dordrecht, The Netherlands: Kluwer), pp. 183–203.
- Deeks, M.J., and Hussey, P.J. (2005). Arp2/3 and SCAR: Plants move to the fore. *Nat. Rev. Mol. Cell Biol.* **6**: 954–964.
- Deeks, M.J., Kaloriti, D., Davies, B., Malho, R., and Hussey, P.J. (2004). *Arabidopsis* NAP1 is essential for Arp2/3-dependent trichome morphogenesis. *Curr. Biol.* **14**: 1410–1414.
- de Graaf, B.H.J., Cheung, A.Y., Andreyeva, T., Lévassieur, K., Kieliszewski, M., and Wu, H.-m. (2005). Rab11 GTPase-regulated membrane trafficking is crucial for tip-focused pollen tube growth in tobacco. *Plant Cell* **17**: 2564–2579.
- Djakovic, S., Dyachok, J., Burke, M., Frank, M.J., and Smith, L.G. (2006). BRICK1/HSPC300 functions with SCAR and the ARP2/3 complex to regulate epidermal cell shape in *Arabidopsis*. *Development* **133**: 1091–1100.
- El-Assal, S.E.D., Le, J., Basu, D., Mallery, E.L., and Szymanski, D.B. (2004). *Arabidopsis* GNARLED encodes a NAP125 homolog that positively regulates Arp2/3. *Curr. Biol.* **14**: 1405–1409.
- Finka, A., Schaefer, D.G., Saidi, Y., Goloubinoff, P., and Zryd, J.P. (2007). In vivo visualization of F-actin structures during the development of the moss *Physcomitrella patens*. *New Phytol.* **174**: 63–76.
- Fowler, J.E., and Quatrano, R.S. (1997). Plant cell morphogenesis: Plasma membrane interactions with the cytoskeleton and cell wall. *Annu. Rev. Cell Dev. Biol.* **13**: 697–743.
- Frank, M., Coumaran, E., Dyachok, J., Djakovics, S., Nolasco, M., Li, R., and Smith, L.G. (2004). Activation of Arp2/3 complex-dependant actin polymerisation by plant proteins distantly related to Scar/WAVE. *Proc. Natl. Acad. Sci. USA* **101**: 16379–16384.
- Frank, M.J., Cartwright, H.N., and Smith, L.G. (2003). Three Brick genes have distinct functions in a common pathway promoting polarized cell division and cell morphogenesis in the maize leaf epidermis. *Development* **130**: 753–762.
- Harries, P.A., Pan, A., and Quatrano, R.S. (2005). Arp2/3 complex component ARPC1 is required for proper cell morphogenesis and polarized cell growth in *Physcomitrella patens*. *Plant Cell* **17**: 2327–2339.

- Ibarra, N., Pollitt, A., and Insall, R.H. (2005). Regulation of actin assembly by SCAR/WAVE proteins. *Biochem. Soc. Trans.* **33**: 1243–1246.
- Kamisugi, Y., Cuming, A.C., and Cove, D.J. (2005). Parameters determining the efficiency of gene targeting in the moss *Physcomitrella patens*. *Nucleic Acids Res.* **33**: e173.
- Kunda, P., Craig, G., Dominguez, V., and Baum, B. (2003). Abi, Sra1, and Kette control the stability and localization of SCAR/WAVE to regulate the formation of actin-based protrusions. *Curr. Biol.* **13**: 1867–1875.
- Le, J., Mallery, E.L., Zhang, C.H., Brankle, S., and Szymanski, D.B. (2006). *Arabidopsis* BRICK1/HSPC300 is an essential WAVE-complex subunit that selectively stabilizes the Arp2/3 activator SCAR2. *Curr. Biol.* **16**: 895–901.
- Lee, K.J.D., Sakata, Y., Mau, S.L., Pettolino, F., Bacic, A., Quatrano, R.S., Knight, C.D., and Knox, J.P. (2005). Arabinogalactan proteins are required for apical cell extension in the moss *Physcomitrella patens*. *Plant Cell* **17**: 3051–3065.
- Li, Y.H., Sorefan, K., Hemmann, G., and Bevan, M.W. (2004). *Arabidopsis* NAP and PIR regulate actin-based cell morphogenesis and multiple developmental processes. *Plant Physiol.* **136**: 3616–3627.
- Machesky, L.M., and Insall, R.H. (1998). Scar1 and the related Wiskott-Aldrich syndrome protein, WASP, regulate the actin cytoskeleton through the Arp2/3 complex. *Curr. Biol.* **8**: 1347–1356.
- Mathur, J. (2005). The ARP2/3 complex: Giving plant cells a leading edge. *Bioessays* **27**: 377–387.
- Mathur, J., Mathur, N., Kirik, V., Kernebeck, B., Srinivas, B.P., and Hulskamp, M. (2003). *Arabidopsis* CROOKED encodes for the smallest subunit of the ARP2/3 complex and controls cell shape by region specific fine F-actin formation. *Development* **130**: 3137–3146.
- Menand, B., Calder, G., and Dolan, L. (2007a). Both chloronemal and caulonemal cells expand by tip growth in the moss *Physcomitrella patens*. *J. Exp. Bot.* **58**: 1843–1849.
- Menand, B., Yi, K., Jouannic, S., Hoffman, L., Ryan, E., Linstead, P., Schaefer, D.G., and Dolan, L. (2007b). An ancient mechanism controls the development of cells with a rooting function in land plants. *Science* **316**: 1477–1480.
- Mullins, R.D., and Pollard, T.D. (1999). Structure and function of the Arp2/3 complex. *Curr. Opin. Struct. Biol.* **9**: 244–249.
- Perroud, P.F., and Quatrano, R.S. (2006). The role of ARPC4 in tip growth and alignment of the polar axis in filaments of *Physcomitrella patens*. *Cell Motil. Cytoskeleton* **63**: 162–171.
- Preuss, M.L., Serna, J., Falbel, T.G., Bednarek, S.Y., and Nielsen, E. (2004). The *Arabidopsis* Rab GTPase RabA4b localizes to the tips of growing root hair cells. *Plant Cell* **16**: 1589–1603.
- Quatrano, R.S., McDaniel, S.F., Khandelwal, A., Perroud, P.-F., and Cove, D.J. (2007). *Physcomitrella patens*: Mosses enter the genomic age. *Curr. Opin. Plant Biol.* **10**: 182–189.
- Rogers, S.L., Wiedemann, U., Stuurman, N., and Vale, R.D. (2003). Molecular requirements for actin-based lamella formation in *Drosophila* S2 cells. *J. Cell Biol.* **162**: 1079–1088.
- Schaefer, D.G. (2001). Gene targeting in *Physcomitrella patens*. *Curr. Opin. Plant Biol.* **4**: 143–150.
- Schaefer, D.G., and Zryd, J.P. (1997). Efficient gene targeting in the moss *Physcomitrella patens*. *Plant J.* **11**: 1195–1206.
- Smith, L.G., and Oppenheimer, D.G. (2005). Spatial control of cell expansion by the plant cytoskeleton. *Annu. Rev. Cell Dev. Biol.* **21**: 271–295.
- Szymanski, D.B. (2005). Breaking the WAVE complex: The point of *Arabidopsis* trichomes. *Curr. Opin. Plant Biol.* **8**: 103–112.
- Takenawa, T., and Suetsugu, S. (2007). The WASP-WAVE protein network: Connecting the membrane to the cytoskeleton. *Nat. Rev. Mol. Cell Biol.* **8**: 37–48.
- Uhrig, J.F., Mutondo, M., Zimmermann, I., Deeks, M.J., Machesky, L.M., Thomas, P., Uhrig, S., Rambke, C., Hussey, P.J., and Hulskamp, M. (2007). The role of *Arabidopsis* SCAR genes in ARP2-ARP3-dependent cell morphogenesis. *Development* **134**: 967–997.
- Vidali, L., Augustine, R.C., Kleinman, K.P., and Bezanilla, M. (2007). Profilin is essential for tip growth in the moss *Physcomitrella patens*. *Plant Cell* **19**: 3705–3722.
- Zhang, X.G., Dyachok, J., Krishnakumar, S., Smith, L.G., and Oppenheimer, D.G. (2005). IRREGULAR TRICHOME BRANCH1 in *Arabidopsis* encodes a plant homolog of the actin-related protein2/3 complex activator SCAR/WAVE that regulates actin and microtubule organization. *Plant Cell* **17**: 2314–2326.